LEGIBILITY NOTICE

A major purpose of the Technical Information Center is to provide the broadest dissemination possible of information contained in DOE's Research and Development Reports to business, industry, the academic community, and federal, state and local governments.

Although a small portion of this report is not reproducible, it is being made available to expedite the availability of information on the research discussed herein.

1

LA-UR -89-2746

CONF-8106201--2

SEP 6 1989

LA-UR--89-2746

DE89 016585

TITLE SHORT WAVELENGTH STRIATIONS ON EXPANDING PLASMA CLOUDS

AUTHOR(S) D. Winske and S. P. Gary

SUBMITTED TO Workshop on Theoretical Geoplasma Physics, Cambridge, MA, June 1987

SHORT WAVELENGTH STRIATIONS ON EXPANDING PLASMA CLOUDS

D. Winske and S. P. Gary

Los Alamos National Laboratory, Los Alamos, NM 87545

ABSTRACT

The growth and evolution of short wavelength (<ion gyroradius) flute modes on a plasma expanding across an ambient magnetic field have been actively studied in recent years, both by means of experiments in the laboratory as well as in space and through numerical simulations. We review the relevant observations and simulation results, discuss the instability mechanism and related linear theory, and describe recent work to bring experiments and theory into better agreement.

I. INTRODUCTION: OBSERVATIONS AND SIMULATIONS

In active experiments substances, such as chemicals (e.g., barium) or energetic particle beams, are released in space and followed in time to investigate the response of the ambient medium and to infer its underlying properties. Notable examples are the AMPTE (Active Magnetospheric Particle Tracer Explorers) releases of barium in the magnetotail, in which optical observations from Earth followed the development of field aligned ripples on the surface of the expanding clouds [1]. Similar surface features, so called prompt striations, were seen in other release experiments in the ionosphere [2]. The waves on the surface can generally be characterized as short wavelength ($<$ ion gyroradius $<$ final cloud size), high frequency (growth rate $>$ ion gyrofrequency), flute ($k_\parallel = 0$) modes. Similar phenomena can be produced in the laboratory by means of a gun [3] or laser generated plasma [4-6] expanding across an externally applied magnetic field. In all cases the instability leads to modest size filaments on the surface, but not to the breakup of the cloud. The striations observed in [4] were similar those seen in the AMPTE releases in that they tended to disappear as the cloud started to recollapse. The structures in [6] were longer lived; the ends of the flutes did not seem to be slowed by the magnetic field, but instead continued to freestream and later sometimes bifurcated. While the wavelengths measured in [3] and [4] varied inversely with the magnetic field ($k \sim B^{\alpha}, \alpha < 1$), those in [6] were independent of B. These observations have led to a vigorous campaign of plasma simulation and theoretical analysis in the last few years (see [7] for a review), the present status of which is updated in this paper.

In addition to the experimental results, numerous computer simulations have helped to elucidate the underlying physics of the instability. Simulations have been carried out with electrostatic [8,9] and electromagnetic particle codes [10,11], hybrid codes (particle ions, fluid electrons) [12,13], and MHD codes with the Hall term [14] in various geometries in both two and three spatial dimensions. The fact that all of these calculations show the development of the instability suggests a robust generation mechanism that is not sensitive to the details of the plasma state. An example of one such simulation [11] is shown in Figure 1, in which are displayed 3 D perspectives of the ion density of a plasma cylinder expanding transverse to an applied magnetic field. As the plasma expands, the density (hence the height of the column) drops and perturbations form on the surface. At later times the outer edges of the perturbations continue to freestream outward, those on the surface coalesce to longer wavelengths, and the central region starts to recollapse. Corresponding pictures for the magnetic field not shown here indicate that in the expansion process the magnetic field is excluded from the center, forming a diamagnetic cavity.

The calculations in Figure . were done with an electromagnetic particle code. Similar calculations in the electrostatic limit [8,9] indicate that the surface modes develop in the ion and electron densities (usually seen first in the electrons), but no magnetic cavity forms. Electromagnetic simulations in which the electrons are treated as a massless fluid [12] also yield instability, but one which grows somewhat more slowly at a wavelength that is determined by the grid size, and a nonlinear state where the filaments can become large enough to break off from the main column. The instability appears to grow somewhat faster when the calculations are carried out in 3-D. The surface modes are also observed in an expanding plasma slab rather than the usual cylinder configuration, using an electromagnetic hybrid code that retains the electron mass [13] as well as in an MHD code in which the Hall term is kept [14]. In the former case the wavelength of the instability is well resolved, while in the latter case it is determined by the grid size; in both situations the unstable modes evolve to longer wavelengths in time. Because the various simulation models emphasize different physics, a number of explanations have been proposed to interpret the numerical results and their relation to the experiments. We next turn to a discussion of the basic instability mechanism and analysis of the wave properties based on linear theory

II. THEORY: INSTABILITY MECHANISM AND LINEAR ANALYSIS

The mechanism by which the instability is excited has become well understood in recent years [7,10,15,16]. Because the spatial and temporal scales of the unstable waves are shorter than those associated with ion gyromotion, the ions are essentially unmagnetized. While unconstrained by the magnetic field, the ions are nevertheless slowed by a radial electric field (E_r) that results from charge separation with the electrons that are strongly tied to the magnetic field. The process is depicted in Figure 2. The ion momentum equation can be rewritten to give an expression for E_r

$$eE_r = m_i \frac{dV_{ir}}{dt} + \frac{T_i}{n_i}\frac{dn_i}{dr} = -m_i g - T_i \epsilon_n \tag{1}$$

where T_i, n_i, and V_{ir} are the ion temperature, density, and radial velocity respectively, and the deceleration $g = -dV_{ir}/dr (> 0)$ and density gradient $\epsilon_n = -n_i^{-1} dn_i/dr (> 0)$ can also be defined. In the presence of the electric field, the electrons drift azimuthally; their $\vec{E} \times \vec{B}$ drift is given by

$$V_E = -\frac{cE_r}{B_o} = \frac{m_i c g}{eB_o} + \frac{T_i c \epsilon_n}{eB_o} = V_g + V_n \tag{2}$$

where B_o is the ambient magnetic field. The relative electron ion drift, which is the free energy source for the instability, thus consists of two terms: V_n, which depends on the ion pressure gradient (T_i assumed constant) and V_g, which is related to the radial deceleration of the ions. In the absence of a radial expansion, the ion pressure gradient driven instability is known as the lower hybrid drift instability. The old papers on this instability (e.g. [17]) do consider the more general case of $V_g \neq 0$, but for their applications $V_g < V_n$ and V_g

was usually ignored. In the case of expanding plasmas, however, the contribution to the electric field from the deceleration can be dominant, and the instability can persist in the limit $V_n = 0$ (e.g., the simulations in [12]). One also noted from Eqs. (1-2) the absence of dependence on electron properties. The radial electric field can arise either from local charge separation effects in full particle simulations or from the quasineutral approximation used in the hybrid code formations.

Instead of concentrating on the radial electric field, one can emphasize the role of the deceleration "g". The fact that the instability results when the deceleration and the density gradient are oppositely directly ($\epsilon_n g > 0$ in the present notation), suggests a physical analogy with the Rayleigh-Taylor instability. However, as pointed out by Hassam and Huba [15,16], the instability here is very different from the usual Rayleigh-Taylor instability: the ions are unmagnetized and the mode is characterized by compressional rather than transverse perturbations. In addition, one can easily get confused about the direction of the deceleration, since the ions are in a non-inertial frame. Thus, it seems preferable to retain the picture of electrons drifting relative to the ions in the azimuthal direction due to a radial electric field that is enhanced by the deceleration of the plasma, even in the limit where the electrons are a charge neutralizing fluid [12-13], or not even explicitly kept in the calculations [14].

Given this picture of the origin of the instability, it is straightforward to derive a linear dispersion equation for perturbations $\sim e^{ik r \theta - \omega t}$, where k is the azimuthal wavenumber (i.e., the direction of V_E) and $\omega = \omega_r + i\gamma$ is the complex frequency. The essential features of the unstable waves can be obtained from a local analysis, assuming cold electrons drifting with velocity V_E relative to unmagnetized ions. For example, in [9,18] the dispersion equation is derived in the electrostatic limit with finite electron temperature, while in [10] cold electrons are assumed, but electromagnetic contributions are included. Figure 3 displays an example of the instability properties obtained from a numerical solution of the local, electromagnetic dispersion equation [10] with $\beta_i = 8\pi n_i T_i/B_o^2 = 0.2$, $T_e = 0$, $V_n/v_A = 1$ ($v_A^2 = B_o^2/4\pi n_i m_i$) and $V_g/v_A = 0$ [left panel] and $V_g/v_A = 3$ [right panel]. The dashed curves correspond to the growth rate, solid curves curves to the real frequency; both are normalized to the ion cyclotron frequency $\Omega_i = eB_o/m_i c$. The wavenumber is normalized to the ion inertial length c/ω_i ($\omega_i^2 = 4\pi n_i e^2/m_i$). The curves in the left panel correspond to the case where g=0 (usual lower hybrid drift instability). The waves are unstable over a broad range of wavenumbers, with maximum growth occurring at short wavelengths, $kc\omega_i \sim 140$, corresponding to $kc/\omega_e = 3.5$ ($m_i/m_e = 1836$). At k corresponding to maximum growth, $\gamma \sim \omega_r \sim 0.7\omega_{LH}$, where the lower hybrid frequency is $\omega_{LH} \simeq (\Omega_e\Omega_i)^{1/2}$. The unstable wave spectrum extends down to $k \rightarrow 0$, where $\gamma \gg \omega_r$. The addition of a nonzero deceleration ($V_g/v_A = 3$, right panel) has a significant effect on the mode structure. The maximum growth rate is now larger (about a factor of two) and occurs at longer wavelength (about a factor of two), while $\omega_r \sim \gamma$ continues to hold at maximum growth. In addition, the growth rate for $kc/\omega \rightarrow 0$ is much larger than when g=0 and ω_r remains very small.

Using the standard argument that the modes with the largest growth rates will grow out of the noise faster to larger amplitude and thus will be the ones observed, linear theory makes definitive predictions concerning the surface structures seen in the AMPTE release and in laboratory experiments. However, the observed striations are often longer in wavelength. For example, in the AMPTE barium release of 21 March [1], there were about 24 evenly spaced flutes on the surface of the barium cloud as it reached its final size, radius $\sim$ 240 km, at a time $\Omega_i t \simeq 1$. Using measured values of the density, this corresponds to a wavenumber $kc/\omega_i \sim 20$ [11]. Linear theory, however, yields a maximum growth rate $\gamma \sim \Omega_{LH} \sim 500\Omega_i$ at $kc/\omega_i \sim 400$. In addition, the time lapsed photographs suggested that the striations were roughly stationary on the surface, imply $\omega_r \simeq 0$, instead of $\omega_r \sim \gamma$, as indicated by the theory. Discrepancies of comparable magnitude exist for experiments involving laser produced plasmas expanding across strong (0.1-1.0T) magnetic fields [6], so that one cannot dismiss the differences as merely due to uncertainties in the parameters (although such uncertainties do exist).

An alternative approach to predicting the mode structure is to start with the observational fact that the wavelengths are long, $kc/\omega_i \sim 1$ and eliminate the electron dynamics first off. The resulting fluid description [15,16] yields a simple dispersion relation that shows $\gamma \sim k$, $\omega_r \simeq 0$, which is consistent with the kinetic treatment in the limit $k \to 0$ [10,16]. However, since the theory only gives the scaling $\gamma \sim k$, some additional physics must still be added to determine the wavelength.

Given the inadequacies of these two approaches, research over the past year has emphasized other effects which can be included in the theory. Progress in some of these areas is outlined in the next section.

III. RECENT IMPROVEMENTS TO THE THEORY

To reconcile the difference between linear theory and the observations, a number of additional effects have been proposed and investigated. We briefly describe a number of these: (A) 3-D effects, (B) nonlocal linear theory, (C) finite beta effects, (D) collisions, (E) nonlinear theory, and (F) electron processes.

A. 3-D Effects

Plasma expansions in three dimensions have been carried out with both electromagnetic particle [19] and massless electron hybrid codes [12]. Compared to 2-D, the instability appears to develop faster and at a slightly longer wavelength. The results are consistent with a larger effective deceleration in three dimensions compared to 2-D. Gisler and Lemons [20] have compared various expansion models (2-D and 3-D expansions everywhere perpendicular to the magnetic field as well as 2-D across the field with free expansion along $\vec{B}$) and concluded that g is about 20% larger in 3-D as compared with 2-D. While not a large effect, it is the direction of bringing the theory and experimental results closer together.

B. Nonlocal Effects

While the linear analysis described in Section II was carried out in the local approximation, it is evident from the simulations (e.g., Figure 1) and observations that the plasma compresses into a shell as it expands. Thus, the inclusion of realistic radial profiles is a natural refinement of the theory. Lemons [21] has done a sharp boundary analysis in the electrostatic limit, while Huba *et al.* [22] have conducted a study based on their modified fluid equations. In the short wavelength limit [21], there is little change: maximum growth occurs at about the same wavelength as in the local treatment. At longer wavelengths both methods yield growth rates γ proportional to $k^{1/2}$ instead of k (which makes the spectrum similar to that of the usual Rayleigh-Taylor instability [16]), as found earlier by Peter *et al.* [23]. However, in the long wavelength limit, while the radial profile can affect the value of the growth rate, the azimuthal wavenumber (i.e., the observed quantity) remains undetermined. One can verify that the growth rate actually varies as $k^{1/2}$ by means of electromagnetic hybrid simulations [12]. When the initial cylinder of plasma expands outward with negligible thermal speed of the ions (compared to an expansion speed of about the Alfven speed), the most unstable mode is the shortest one allowed by the grid, $\gamma \sim k_m^{\alpha}$, where k_m is the maximum wavenumber $\sim$ inverse of the grid spacing. Figure 4 shows the results of several simulations with identical initial conditions, varying only the grid spacing. It is evident that $\gamma \sim k_m^{1/2}$, rather than $\gamma \sim k_m$, consistent with the nonlocal scaling.

C. Finite β_e Effects

Another logical extension of the linear theory is to include finite β_e corrections, as has been done previously for the lower hybrid drift instability [24]. With $g \neq 0$, this remains a straightforward, but tedious task [25]. Analogous to the g=0 results, the effects of finite β_e when $g \neq 0$ play a relatively minor role. They tend to reduce the growth rate at short wavelength and have less effect on γ as $k \to 0$. One suprise is an enhancement in growth at small k in some parameter regimes [25], which may actually lie on a different branch of the dispersion equation, perhaps related to the usual (magnetized ion) Rayleigh-Taylor instability. Because finite β effects tend to reduce the growth rate, one has to be careful that the assumption of unmagnetized ions is not violated ($|\omega| > \Omega_i$). This difficulty can be avoided by going to a Gordeyev representation for the ions [24,26] which allows one to cross smoothly from the unmagnetized to the magnetized regime. Overall, such additions to linear theory give one a more complete and consistent picture of the mode structure, but do little to reduce the differences between predicted and observed wave properties.

D. Collisions

The effect of collisions between the expanding plasma and a background is also interesting and readily adaptable from previous work on the lower hybrid drift instability [27]. While not relevant to the AMPTE barium releases (the waves being seen long after the barium was ionized), collisional effects may be important at early times in releases in the ionosphere [2] and can be simulated in the laboratory [6]. The effect of collisions of electrons with neutrals or ions is to reduce the growth rate of the instability, the largest reduction occurring near k corresponding to maximum growth without collisions, with smaller reductions at longer wavelengths. The wavenumber corresponding to maximum growth is not affected. Collision frequencies well in excess of the linear growth rate are needed to quench the instability. Collisions involving ions with neutrals or electrons enter in two ways. First, as with electron collisions they reduce growth rates, but only small amounts (ion collision frequency $\ll$ linear growth rate without collisions) are needed to quench the instability. More significantly, ion collisions act to oppose the charge separation electric field; they thus tend to reduce g, hence lowering the maximum growth rate and shifting it to shorter wavelengths.

Collisional effects can also be studied by means of simulations. Figure 5 shows ion density contours from three 2-D electromagnetic particle simulations. The left panel is from a run with no collisions and shows a well developed flute instability. The middle panel is from a similar run but where electron (Krook model) collisions have been added in. The instability is still present, but weaker, and the cloud is more diffuse. Ion collisions have been included in the simulation in the right panel; the instability has been suppressed. Collisional effects on the instability have also been investigated in the laboratory by varying the background gas pressure in laser produced expansions [6]. As the background gas pressure is raised (increasing the collision frequency), the surface structures remain at about the same wavelength, but become fainter and eventually disappear, in qualitative agreement with theory.

E. Nonlinear Theory

Nonlinear processes have also been studied, and given that the linear effects discussed above do not bring experiments and theory into agreement, they remain the most promising way of explaining the differences. The main nonlinear effects involve trapping of the ions and nonlinear mode coupling, similar to that which is observed for the g=0 lower hybrid drift instability [28]. The principal difference when the cloud is expanding is that the deceleration of the ions maintains the radial electric field and thus continues to drive the instability by keeping the azimuthal electron-ion drift large. The electric field fluctuations that result from the instability can then become larger than those needed to trap the ions [10]. Thus, mode coupling to longer wavelengths becomes the most important nonlinear effect. Figure 6 shows a time sequence of azimuthal profiles of ion density fluctuations from the simulation displayed in Figure 1. One sees the growth of short wavelength modes that coalesce to longer wavelengths at later times. From the motion of the phase fronts one can also infer the real frequency of the dominant mode is about ω_{LH} at early times [11], but becomes almost zero near the end of the expansion. Numerous other runs over a range of parameters yield similar results and show that the amount of coalescence achieved (i.e., the ratio of the dominant nonlinear wavelength to the dominant linear wavelength) is only about a factor of two or three. However, because the particle simulations follow the complete electron dynamics, one is constrained to a rather narrow parameter space and in particular the product of the time for the cloud to reach its maximum radius (t_c) and the maximum linear growth rate is small, $\gamma t_c < 10$, whereas in the experiments $\gamma t_c > 10^4$. Thus, in the actual experiments there is much more time (as well as several orders of magnitude more linear wavelengths on the surface) before the expansion stops, which can allow mode coupling to proceed further. Recently, Hassam *et al.* [29] have developed a mode coupling theory to model this process. The essence of their model is that are two fundamental wavenumbers: a long wavenumber k_1 corresponding to growth of the waves and scattering of the particles at short wavelength and a small wavenumber k_2 related to long wavelength dissipation. Mode coupling occurs in this system with a nonlinear state dominated by $k_{NL} \sim (k_1 k_2)^{1/2}$. Recalling the characteristics of the AMPTE barium release, if we associate k_1 with that of the most unstable linear mode ($k_1 c/\omega_i \sim 400$) and take $k_2 c/\omega_i \sim 1$, where the instability is stabilized by ion gyroradius effects, one gets $k_{NL} c/\omega_i \sim 20$, consistent with the observations. While no means conclusive as yet, this mode coupling approach does at least seem very promising

It should also be noted that the key parameter for determining the importance of non linear effects seems to be ρ_i/R_B, the ratio of the ion gyroradius using the initial directed velocity of the ions to the final expansion radius of the cloud [11]. When $V_g > V_n$, V_E is proportional to ρ_i/R_B, so that it is some measure of the free energy for the instability. The laboratory experiments [4-6] and the AMPTE barium releases [1], where significant growth of the waves occurs, are characterized by $\rho_i/R_B \geq 1$. On the other hand, naturally occurring diamagnetic cavities are observed infrequently upstream of the bow shock [30]. The spacecraft data yield little evidence for surface waves of significant amplitude or associated plasma heating; in this case $\rho_i/R_B < 0.1$. Particle simulations [11] carried out over a range of ρ_i/R_B also indicate that the instability develops smaller surface filaments as ρ_i/R_B is reduced, while laser experiments [5] suggest that significant anomalous diffusion, implying a strong instability, occurs only for $\rho_i/R_B > 1$.

F. Electron Processes

Finally, we address the question of other physics that may be going on at very early times in the expansion of the cloud. In particular, we examine processes due exclusively to the electrons, before ion dynamics comes into play. While there is no experimental evidence to support the existence of such effects, electron scale processes would occur very rapidly over short distances and would probably not be detected unless great care were exercised. Because the radial electric field is not uniform, one expects V_E to have some radial structure, and in particular a shear which could drive a Kelvin Helmholtz instability on the surface. Sydora *et al.* [8] have attributed the waves seen in their electrostatic simulations to such an effect and Galvez *et al.* [9] detect high frequency waves in their simulation at early time that have been modeled via a Kelvin-Helmholtz analysis including the effect of ions [7]. Barnes *et al.* [19] have shown that the high frequency flute ("piccolo") instability in their electromagnetic particle simulations is not due to the ions by reproducing the instability when the ion to electron mass ratio is increased by 10^5. The extension of their calculations to 3 D shows the piccolo instability may be responsible for the jetting of some electrons out of the cloud along the ambient magnetic field at early times in the expansion. But whether these electron processes can have some effect on the ion dynamics at later times remains to be determined.

IV. CONCLUSIONS

The development of short wavelength flute modes on plasma clouds expanding into a magnetic field have become well understood in the last few years. The mechanism by which the instability is generated and appropriate linear theory, which now includes nonlocal, finite beta, and collisional effects, are well in hand. And good progress is being made in developing a nonlinear mode coupling theory that offers the best hope of resolving the remaining differences between theory and observations. Additional verification and testing of this predictive capability should be encouraged, including reevaluation of previous active experiments, modeling of new laboratory data, and application to future space missions such as CRRES.

ACKNOWLEDGEMENTS

Useful discussions with Drs. K. Akimoto, C. W. Barnes, M. E. Jones, V. A. Thomas, and J. M. Wallace are gratefully acknowledged. We also wish to thank Dr. Thomas for producing Figure 4. This work was performed under the auspices of the U. S. Department of Energy and supported by the Defense Nuclear Agency and NASA.

REFERENCES

1. P. A. Bernhardt, R. A. Roussel-Dupre, M. B. Pongratz, G. Haerendel, A. Valenzuela, D. A. Gurnett, and R. R. Anderson, J. Geophys. Res., **92**, 5777 (1987).

2. E. M. Wescott, H. C. Stenback-Nielsen, T. J. Hallinan, C. S. Deehr, J. V. Olson, J. G. Roederer, and R. D. Sydora, Geophys. Res. Lett., **7**, 1037 (1980).

3. H. Dickinson, W. H. Bostick, J. N. DiMarco, and S. Koslov, Phys. Fluids, **5**, 1048 (1962).

4. S. Okada, K. Sato, and T. Sekiguchi, Japan J. Appl. Phys., **20**, 157 (1981).

5. Yu. P. Zakharov, A. M. Orishich, A. G. Ponomarenko, and V. G. Posukh, Sov. J. Plasma Phys., **12**, 674 (1986).

6. B. H. Ripin, E. A. McLean, C. K. Manka, C. Pawley, J. A. Stamper, T. A. Peyser, A. N. Mostovych, J. Grun, A. B. Hassam, and J. D. Huba, Phys. Rev. Lett., **59**, 2299 (1987).

7. K. Akimoto, M. Galvez, S. P. Gary, A. G. Sgro, and D. Winske, J. Geomag. Geoelect., **40**, 1161 (1988).

8. R. D. Sydora, J. S. Wagner, L. C. Lee, and E. M. Wescott, Phys. Fluids, **26**, 2986 (1983).

9. M. Galvez, S. P. Gary, C. Barnes, and D. Winske, Phys. Fluids, **31**, 1554 (1988).

10. D. Winske, J. Geophys. Res. **93**, 2539 (1988).

11. D. Winske, Phys. Fluids B, **1**, in press (1989).

12. S. H. Brecht and V. A. Thomas, Comput. Phys. Comm., **48**, 135 (1988).

13. A. G. Sgro, S. P. Gary, and D. S. Lemons, Phys. Fluids B, **1**, in press (1989).

14. J. D. Huba, J. G. Lyon, and A. B. Hassam, Phys. Rev. Lett., **59**, 2971 (1987).

15. A. B. Hassam, and J. D. Huba, Geophys. Res. Lett., **14**, 60 (1987).

16. A. B Hassam and J. D. Huba, Phys. Fluids, **31**, 318 (1988).

17. R. C. Davidson and N. T. Gladd, Phys. Fluids **18**, 1327 (1975).

18. S. Okada, K. Sato, and T. Sekiguchi, J. Phys. Soc. Japan., **46**, 355 (1979).

19 C. W. Barnes, M. E. Jones, and D. Winske, in preparation (1989).

20 G. Gisler and D. S. Lemons, J. Geophys. Res , **94**, in press (1989)

21. D S. Lemons, Phys. Fluids B, **1**, 1539 (1989)

22. J. D. Huba, A. B. Hassam, and P. Satyanarayana, Phys. Fluids B, **1**, 931 (1989).

23. W. Peter, A. Ron, and N. Rostoker, Phys. Fluids, **26**, 2276 (1983).

24. R. C. Davidson, N. T. Gladd, J. D. Huba, and C. S. Wu, Phys. Fluids **20**, 301 (1977).

25. J. D. Huba, *et al.*, in preparation (1989).

26. S. P. Gary and J. J. Sanderson, Phys. Fluids, **22**, 1500 (1979).

27. S. P. Gary, P. A. Bernhardt, and T. E. Cole, J. Geophys. Res. **88**, 2103 (1983).

28. J. F. Drake, P. N. Guzdar, A. B. Hassam, and J. D. Huba, Phys. Fluids, **27**, 1148 (1984).

29. A. B. Hassam, *et al.*, in preparation (1989).

30. M. F. Thomsen, J. T. Gosling, S. A. Fuselier, S. J. Bame, and C. T. Russell, J. Geophys. Res., **91**, 2961 (1986).

FIGURE CAPTIONS

Figure 1. Results of an electromagnetic particle simulation showing the ion density at various times of a plasma cylinder expanding in 2-D transverse to a magnetic field.

Figure 2. Schematic of the instability mechanism, showing the radial expansion of the ions, the radial electric field, and the azimuthal drift of the electrons.

Figure 3. Results of linear theory showing real frequencies (solid curves) and growth rates (dashed curves) versus wavenumber for: [left panel] no deceleration, $V_g = 0$, and [right panel] $V_g = 3v_A$.

Figure 4. Results of a hybrid simulation showing growth rate versus k_m ($\sim$ inverse of the grid spacing); $\gamma \sim k_m^{1/2}$ confirms the scaling of the nonlocal theory.

Figure 5. Results of electromagnetic particle simulations showing ion density contours at the same time from different runs: [left] no collisions, [center] electron collisions added, [right] ion collisions included.

Figure 6. Density perturbations on the surface of the expanding cloud shown in Figure 1 versus azimuthal angle at various times showing coalescence of the modes.

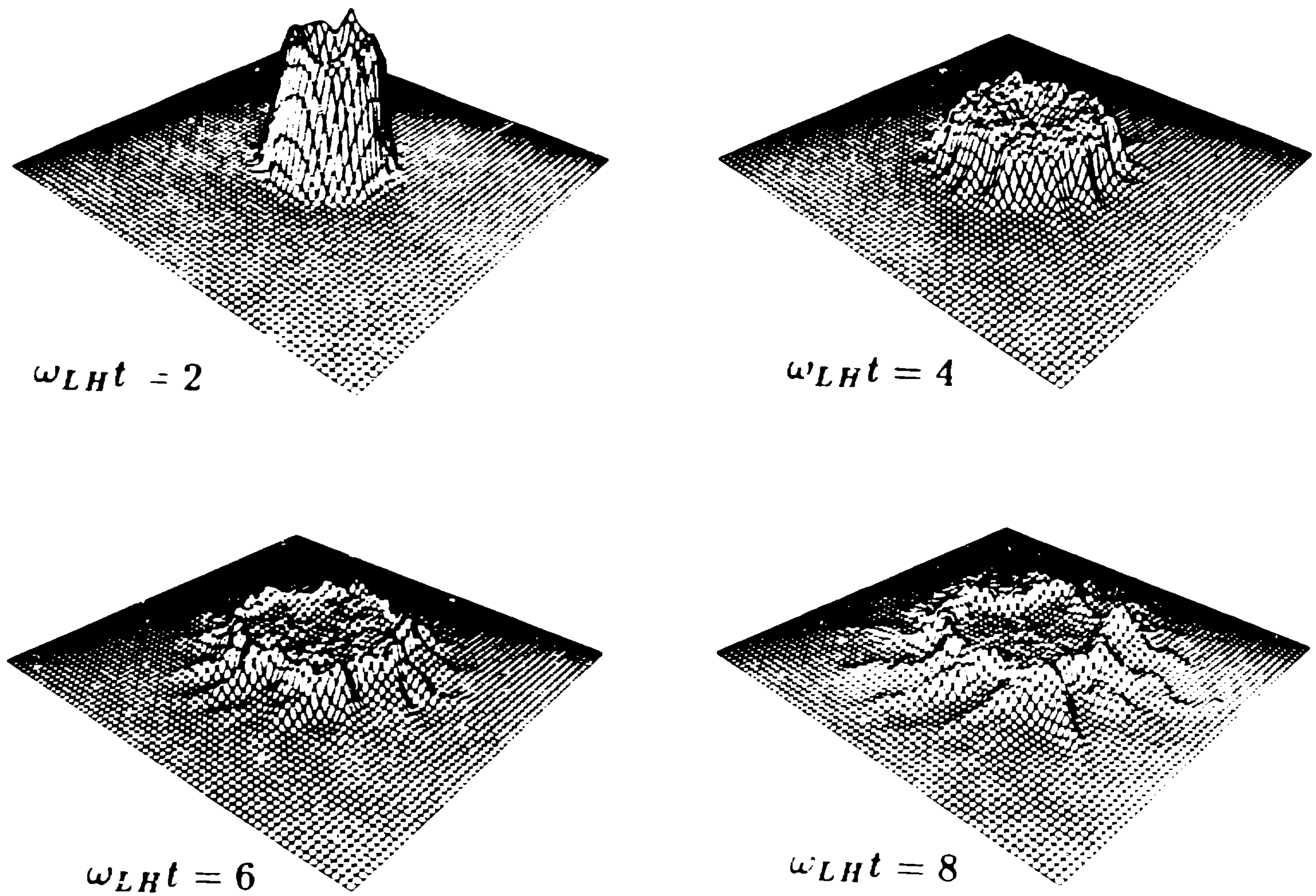

Figure 1

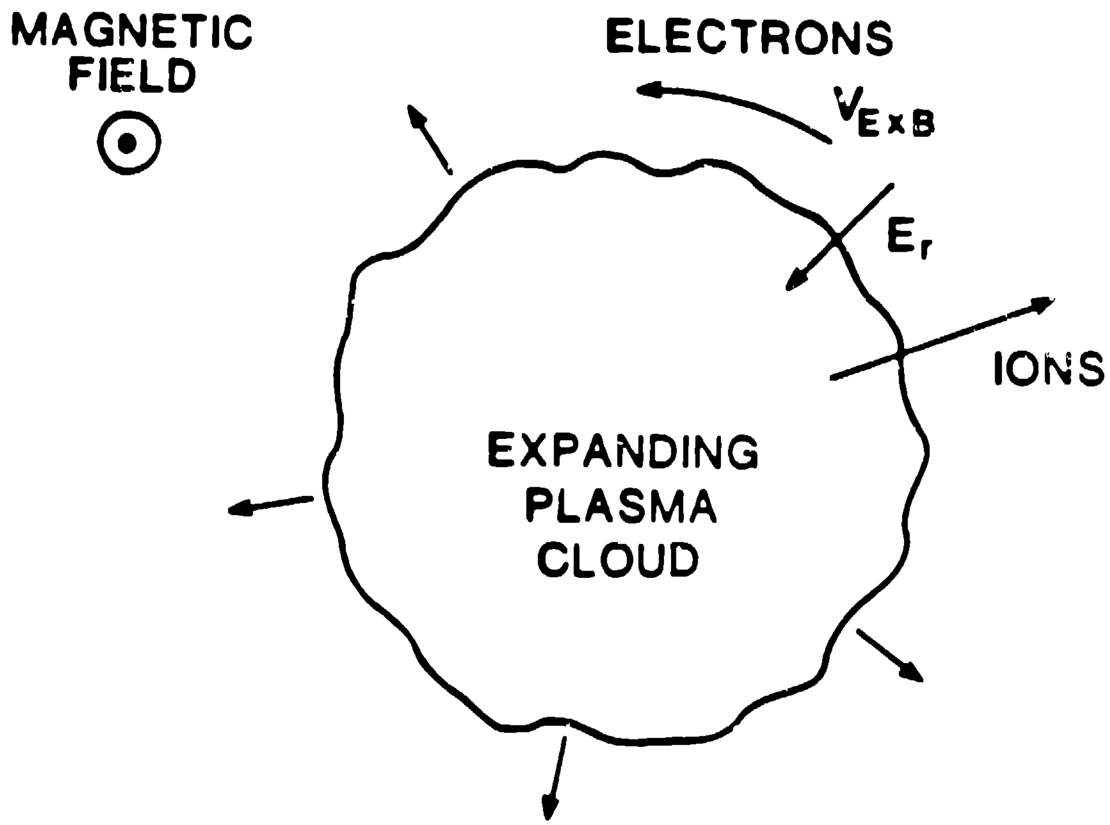
MAGNETIC
FIELD
ELECTRONS
$V_{E \times B}$
E_r
IONS
EXPANDING
PLASMA
CLOUD

Figure 2

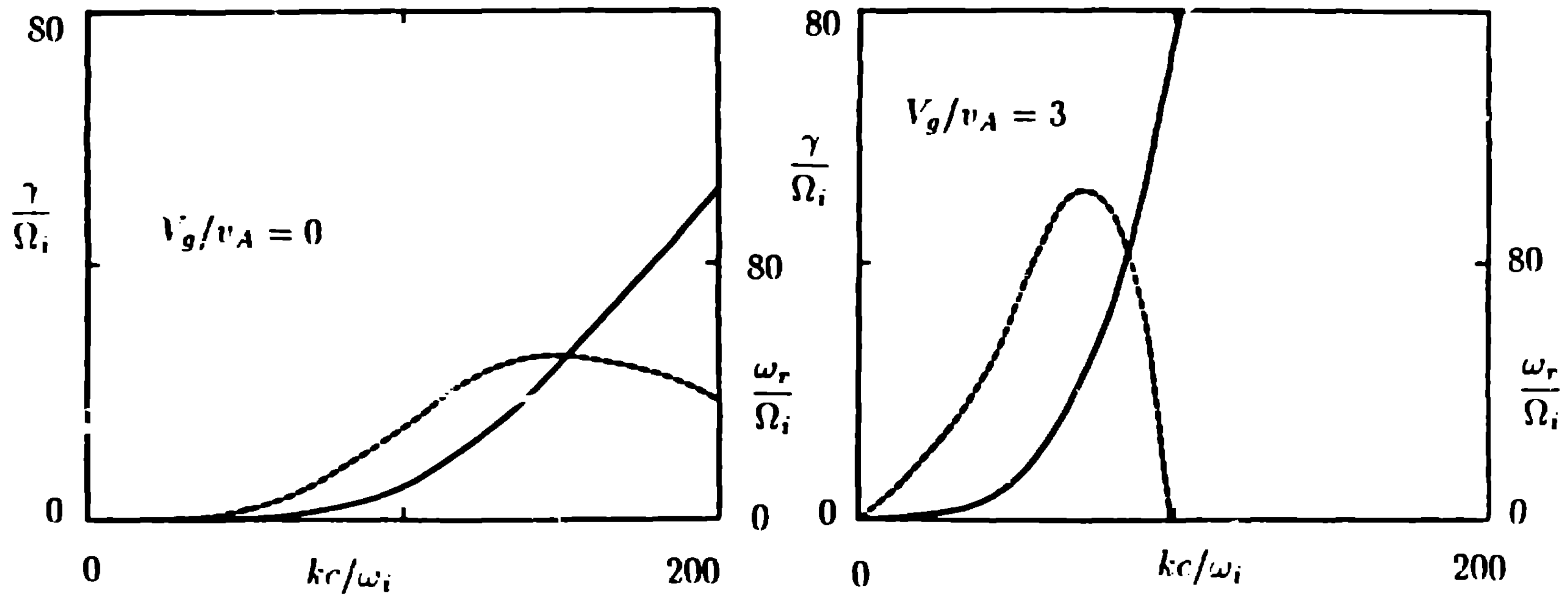
80
γ/Ω_i
V_g/v_A = 0
80
ω_r/Ω_i
0
0
0
kc/ω_i
200
80
V_g/v_A = 3
γ/Ω_i
80
ω_r/Ω_i
0
0
0
kc/ω_i
200

Figure

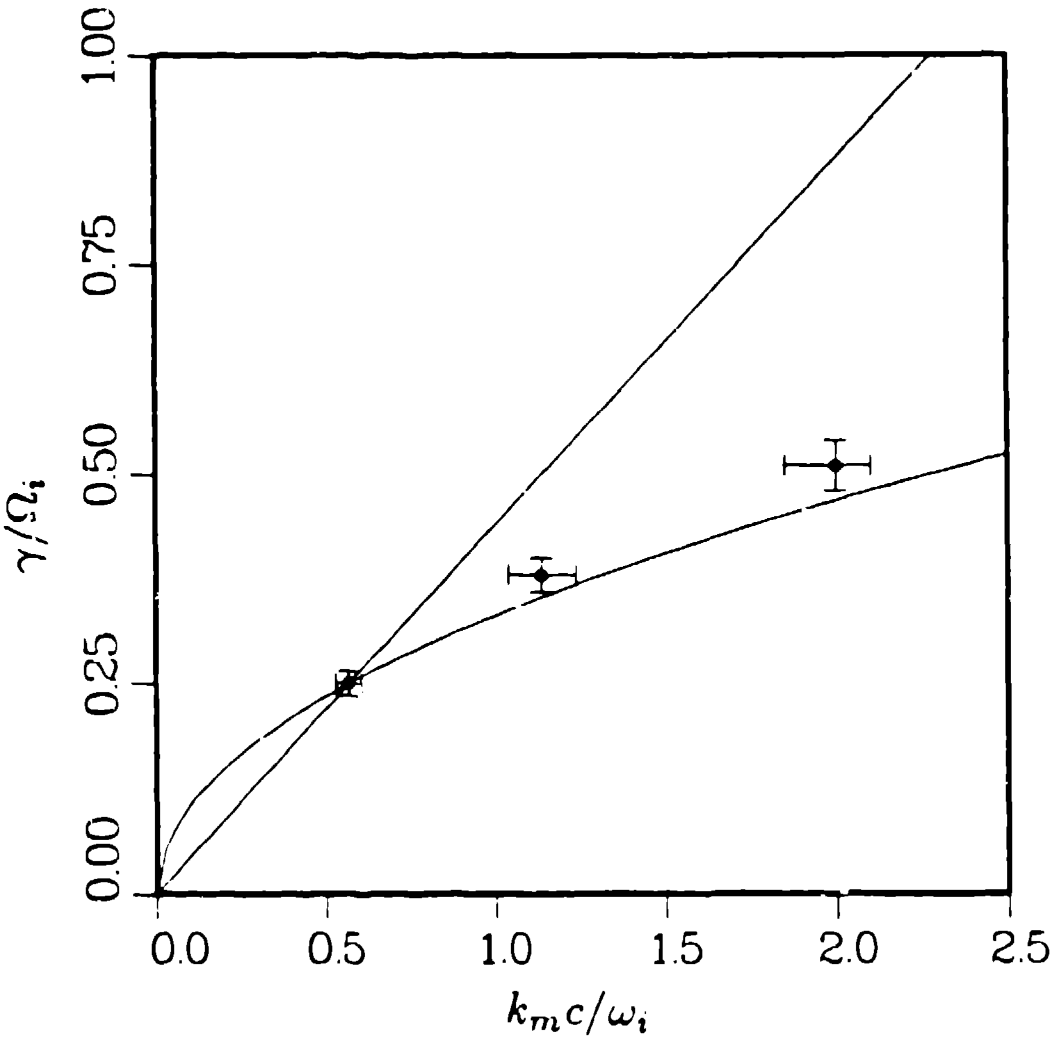

Figure 4

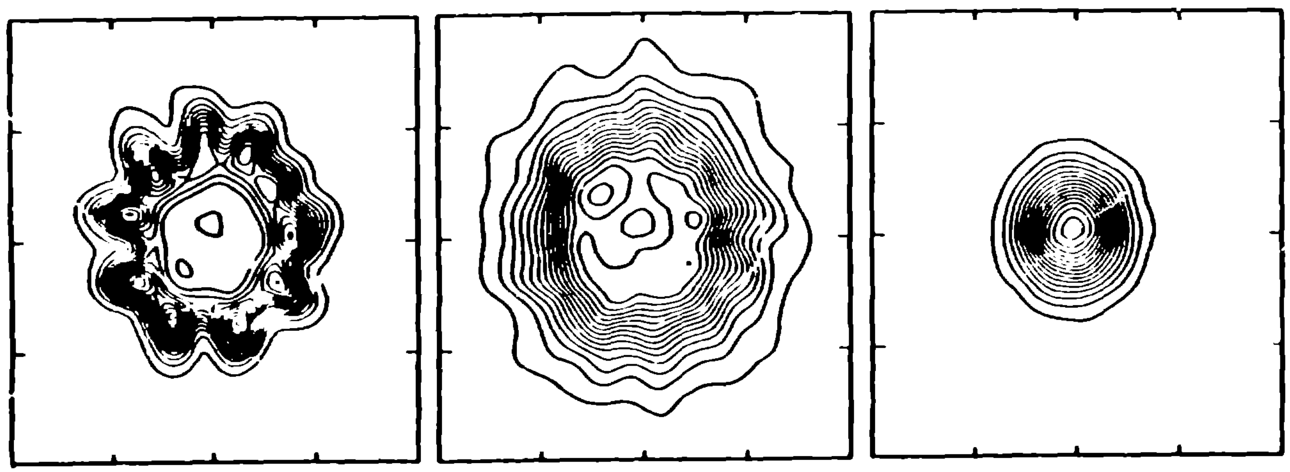

Figure 5

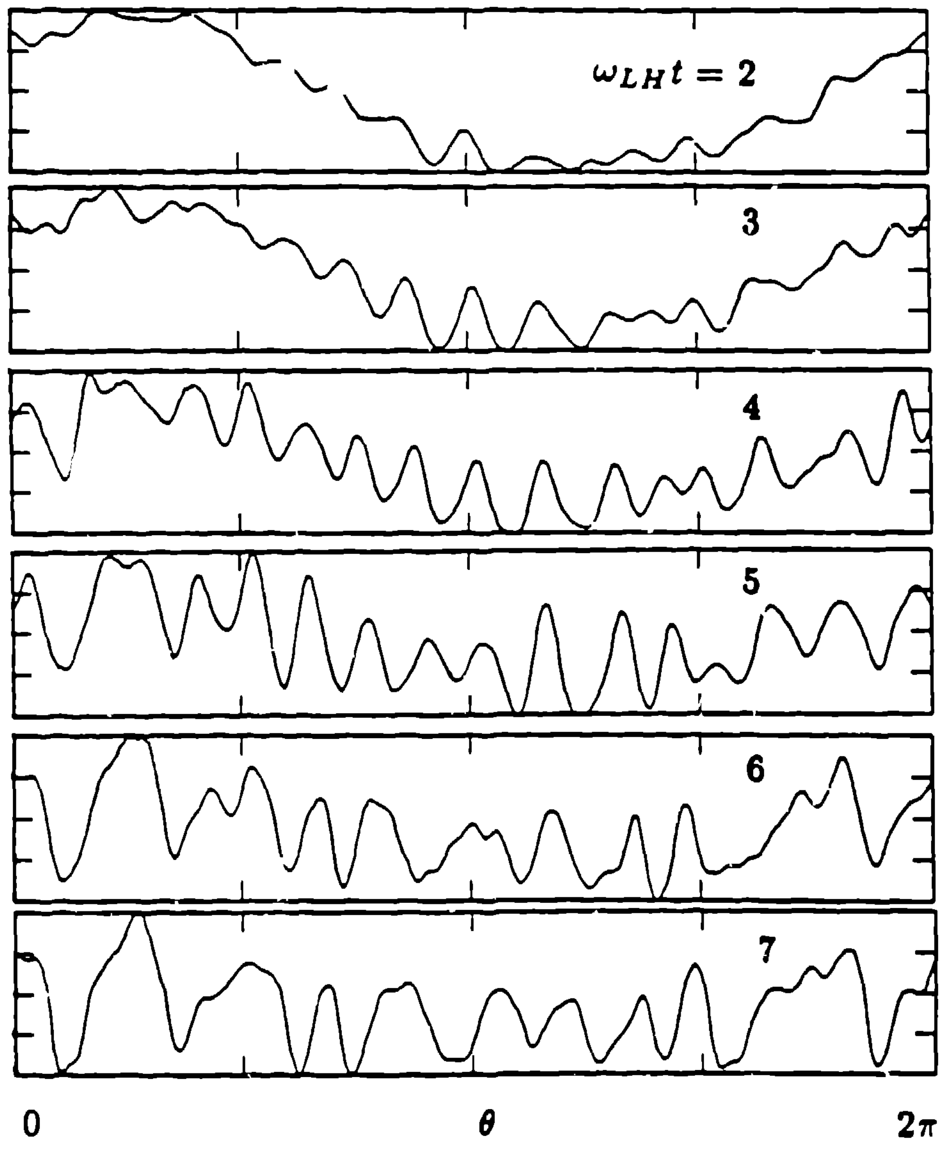

Figure 6